SUPPORTING INFORMATION

Disentangling the effects of temperature and rainfall on the population dynamics of Kalahari meerkats

Oikos

Thorley, J., Duncan, C., Gaynor, D., Manser, M.B. and Clutton-Brock, T.

Table of Contents

Section 1. Correlation between onsite and remotely sensed weather variables.

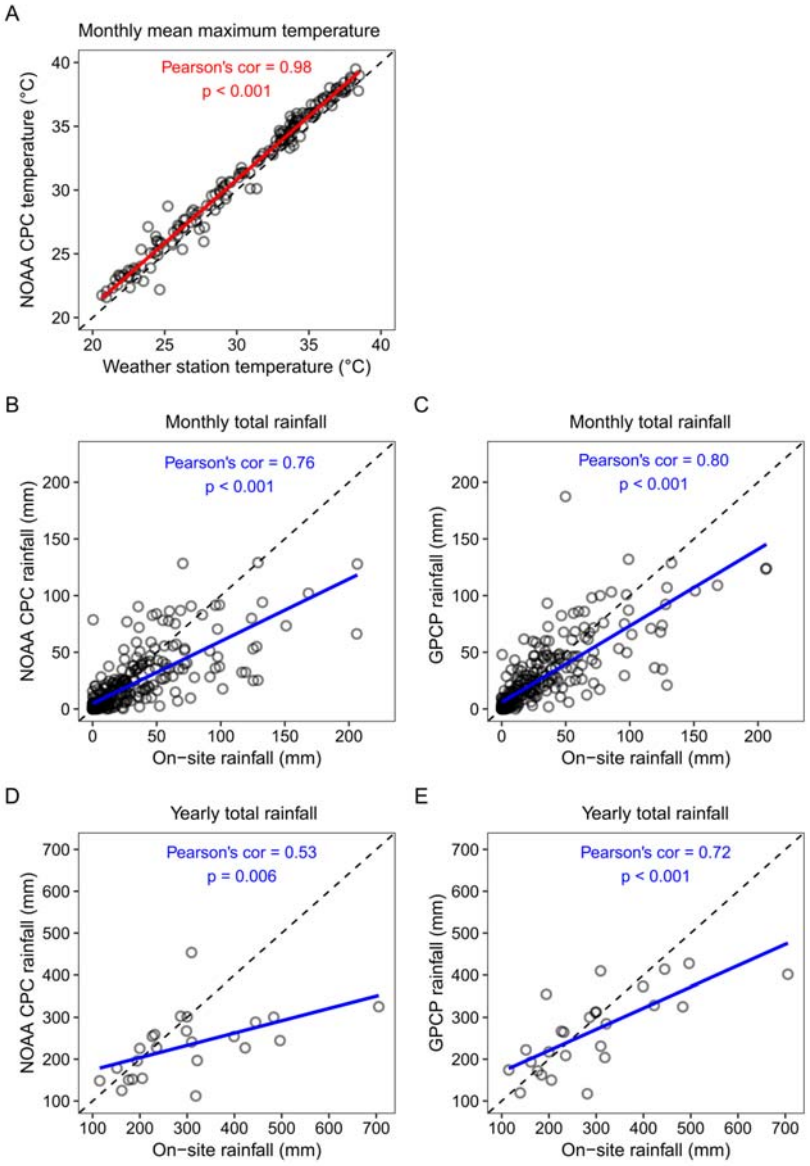

Figure S1.1 Correlations between weather variables measured onsite and equivalent variables obtained through remote sensing: for monthly temperatures (A), monthly rainfall (B, C) and annual rainfall (D, E). Here, temperature refers to the mean maximum daily temperature in each month, while rainfall refers to the total monthly or annual totals, where each annual period covers a single breeding season from July 1st of one year to June 30th of the following year. Onsite temperature data were collected by a weather station from 2010 onwards, whereas onsite rainfall data were collected manually before 2010 (manual rain gauge), and automatically thereafter (weather station). The NOAA CPC product provided temperature and rainfall data at daily resolution, which was then aggregated to monthly or annual resolution. The Global Precipitation Climatology Project v3.2 (GPCP; Huffman et al. 2023) provided data at monthly resolution. The rainfall data from the CPC and GPCP products integrate information from multiple sources, including rain-gauge measurements.

Section 2. Annual vegetation productivity over time and its association with rainfall.

While rainfall measured onsite was positively correlated with rainfall taken from two remote sensing datasets (Section 1), the strength of the correlation varied across datasets (Figure S1.1). As the accurate measurement of rainfall is likely to affect demographic analyses that include rainfall, we compared the ability of each of annual rainfall dataset to predict annual variation in vegetation productivity at our field site, working under the assumption that rainfall in the Kalahari should be highly correlated with vegetation productivity. As rainfall in the region is highly localised, we expected that site-measured rainfall would best predict vegetation productivity.

We extracted vegetation productivity as satellite-derived NDVI (normalised difference vegetation index) values from the MODIS MOD13Q1 product. These data are provided every 16 days on a 250-meter grid and were downloaded using the `MODISTools` R package (Hufkens, 2022).

NDVI values vary over short spatial scales at our field site according to habitat (Figure S2.1). The site covers a section of the dried-up Kuruman River around which are found a diverse landscape of dry pans, vegetated sand dunes, and arid bushveld. Meerkats are selective in their use of these habitats (Turbé, 2006), and the phenology of growing seasons of the habitats differ from one another. Generally, the regions of calcareous sand in and around the riverbed display larger vegetation flushes than the surrounding areas of red sand. By plotting the average NDVI in areas of active space use since 2002, there is a single growing season in each year, and this growing season varies in magnitude and duration. The growing season typically commences in early January and peaks in early March, coinciding closely with the onset of summer rains.

To get a measure of annual productivity across the study site, we clipped the NDVI data to the extent of the population's range and treated each pixel as a separate time series. We then calculated the annual vegetation productivity at each pixel as the Small Integral Value of NDVI (SIV of NDVI) using the TIMESAT software v3.3 (Jönsson & Eklundh, 2004). The software uses an adaptive smoothing algorithm to identify various attributes of productivity time series (Figure S2.2), one of which is the small integral value of vegetation productivity (h). The SIV of NDVI captures the total area under the NDVI curve between the start and end of the growing season, above the baseline NDVI level. It thus measures the total vegetation production of each pixel within a growing season. As NDVI is correlated with photosynthetic activity, NDVI summed over the growth season can be used as an estimate of net primary productivity. It should be noted that some studies prefer to use the SIV of enhanced vegetation index (EVI) to quantity growing season dynamics. However, for our area of the Kalahari, where plant biomass is relatively low, cloud cover is uncommon, and free-standing water is absent, NDVI and EVI are very highly correlated. We therefore chose to use NDVI as it is more widely known amongst animal ecologists. The SIV of NDVI/EVI has been applied in various arid regions of Africa (Wessels et al., 2011; Fensholt et al., 2013), including in the Kalahari Desert (Tokura et al., 2018).

For the adaptive smoothing algorithm, we chose season start and end thresholds of 30% and 20% and used a [half-]window width of 4 for Savitsky-Golay filtering. We used a median filter for the spike method and chose three iterations for the upper envelope adaptation with an adaptation strength of 2. We also forced a minimum NDVI value of 0.135 to filter out a very small number of spuriously low values. We chose these parameters after visually inspecting the impact of different thresholds in the software's MATLAB interface. For each

breeding/growing season, we averaged the SIV of NDVI across all pixels falling within the bounded area to provide a measure of the average vegetation productivity across the area inhabited by the meerkat population. It is this average productivity value that we use going forwards.

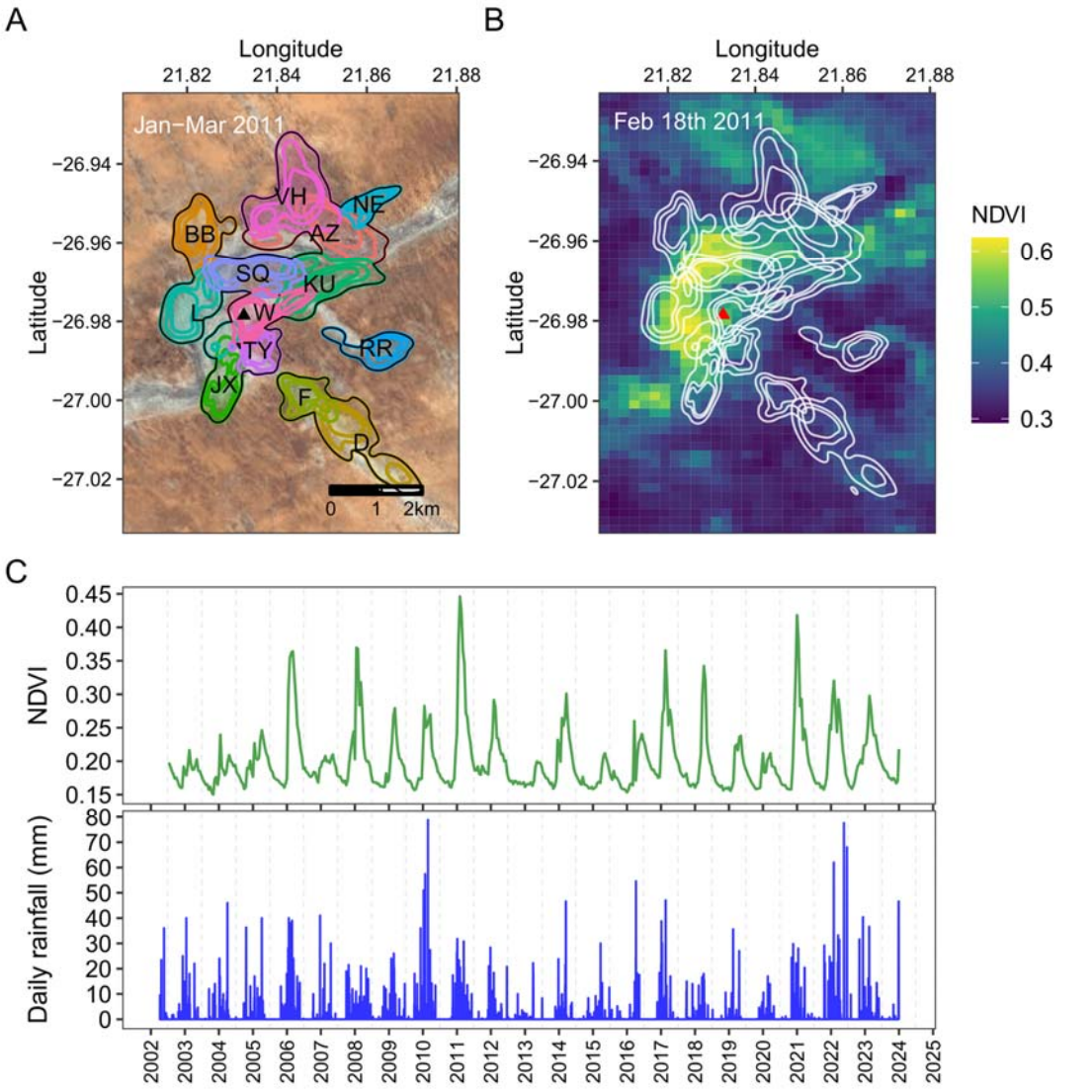

Figure S2.1 NDVI in space and time. (A) Population density was calculated from the home ranges of individual groups in rolling 3-month windows. The home ranges of 12 established groups are shown for a representative window, the contours noting the 95, 75 and 50% KDEs. The aggregation of the home ranges (within black lines) demarcated a total population area over which population density was calculated and used in other parts of our study. (B) NDVI at one point in time. NDVI values vary over short spatial scales in and around the study area. For each 16-day period, the mean NDVI across all pixels that overlapped with the home ranges of frequently visited meerkat groups was calculated and plotted in the time series below. (C) NDVI (green) and rainfall (blue) time series. The rainfall time series is plotted beneath the NDVI time series to demonstrate the close link between vegetation phenology and rainfall. Daily rainfall data were collected onsite.

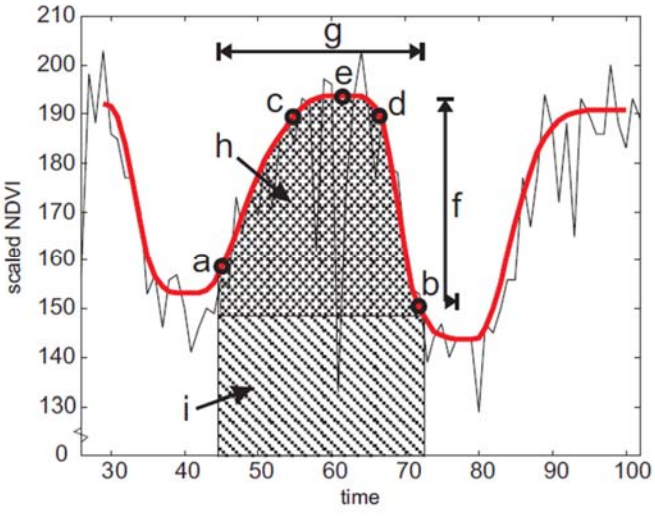

Figure S2.2. Phenological and productivity metrics provided by TIMESAT. Points (a) and (b) mark, respectively, start and end of growing season. Points (c) and (d) give the 80% levels. (e) displays the point with the largest values. (f) displays the seasonal amplitude and (g) the season length. Finally, (h) and (i) are integrals showing the cumulative effect of vegetation growth during the season. Image and text taken from the TIMESAT manual. The time scale will typically be on the order of weeks.

Section 2 Results

Annual rainfall was correlated with the SIV of NDVI for all rainfall datasets (Figure S2.3). The correlation was strongest for the onsite rainfall dataset (Pearson's r = 0.72 [95%CI: 0.44, 0.87], df = 21, p < 0.001), of intermediate strength for the GPCP dataset (Pearson's r = 0.56 [95%CI: 0.20, 0.79], df = 21, p = 0.005), and weakest for the CPC dataset (Pearson's r = 0.45 [95%CI: 0.05, 0.73], df = 21, p = 0.04). The onsite data outperformed the two remotely sensed datasets and unlike them, also generated no obvious outlier seasons, whereas the low of rainfall season of 2022/2023 in the remotely sensed datasets is probably inaccurate for our specific location. The onsite rainfall data also identified the lowest rainfall season of 2012/2023 – when the meerkat population crashed – as having the lowest primary productivity.

The productivity of the vegetation across our study area will also be affected by the magnitude and frequency of effective rainfall pulses (Ogle & Reynolds, 2004), but for our purposes, the total annual rainfall is sufficient to capture key demographic processes. As annual rainfall was highly variable between years, so too was the SIV of NDVI (Figure S2.3D).

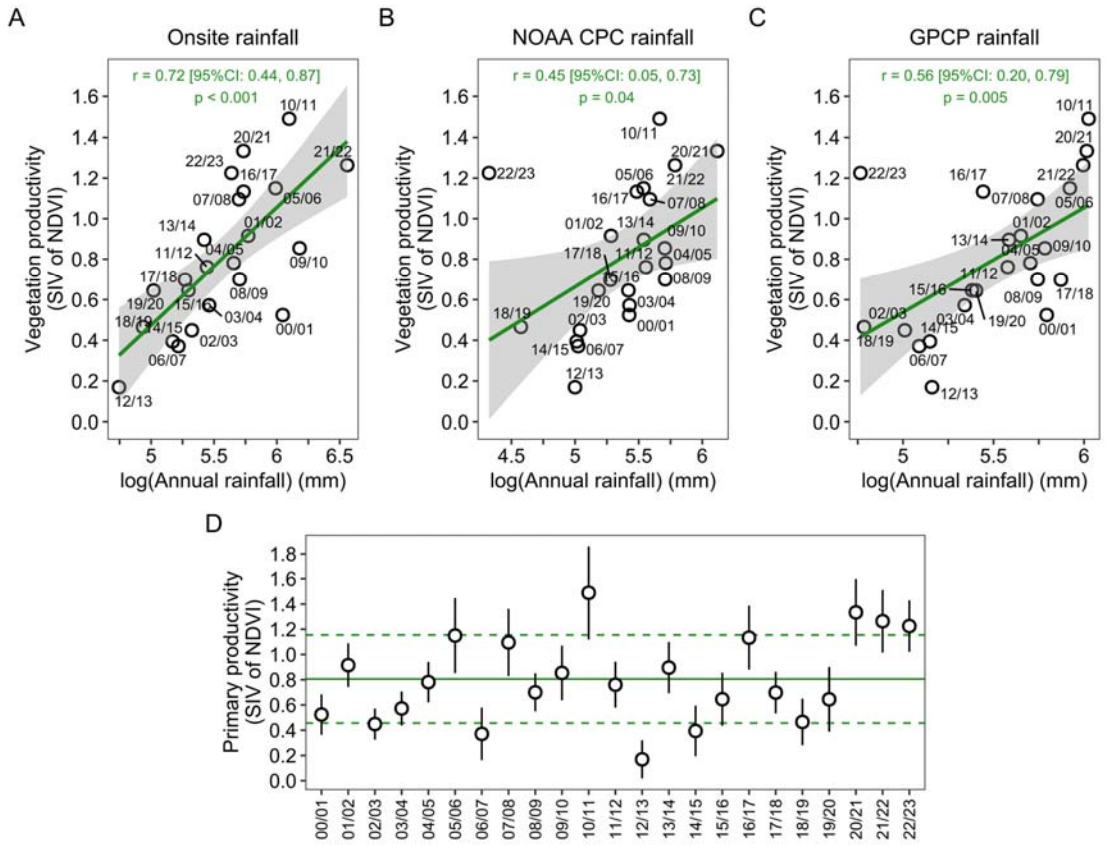

Figure S2.3. Correlations between annual rainfall measures and the primary productivity of vegetation across the study area. The correlation was made with annual rainfall measured either onsite (A), using the CPC product (B), or using the GPCP product (C). (D) Annual vegetation productivity over time. In all figures, the points display the mean SIV of NDVI over all pixels in each growing season. In the lower panel 1 standard deviation of the mean is included as an error bar for each season. The long-term annual mean ± SD are shown by the horizontal solid and dashed lines.

Section 3. Sensitivity analysis for the estimation of home range sizes.

The aim of the analysis was to investigate the effect of sampling effort on the estimation of meerkat home range sizes. Meerkat home ranges are known to be relatively stable over monthly time periods, and previous work has stated that 3 months provides an adequate window over which to estimate stable home ranges (Kranstauber et al., 2019). However, habituated groups that are visited relatively infrequently over a three-month period will provide relatively fewer GPS data than those visited regularly, and it is likely that the estimated home ranges of these under-sampled groups will be lower simply by virtue of the reduced sampling effort.

To examine how sampling effort affects the estimate of home range size, we first calculated the amount of GPS data collected at each group in rolling 3-month windows (e.g. Dec 2011-Feb 2012, Jan 2012-Mar 2012 etc…). Variation in the number of GPS points collected in each period was largely a consequence of the number of times a group was visited, rather than due reduced sampling rates per (the number of fixes per session; Figure S3.1). There were a handful of exceptions - high-rate sessions - that appear in the right-hand tail of the distributions in the upper left panels. However, for the most part, the main difference between periods with high versus low amounts of data was the number of sessions that the group provided GPS data. With this knowledge, we can leverage the periods with high amounts of data to estimate the effect of increasing sample size (i.e., the number of sessions visited in a period) on home range size, by resampling across a range of sample sizes (sessions).

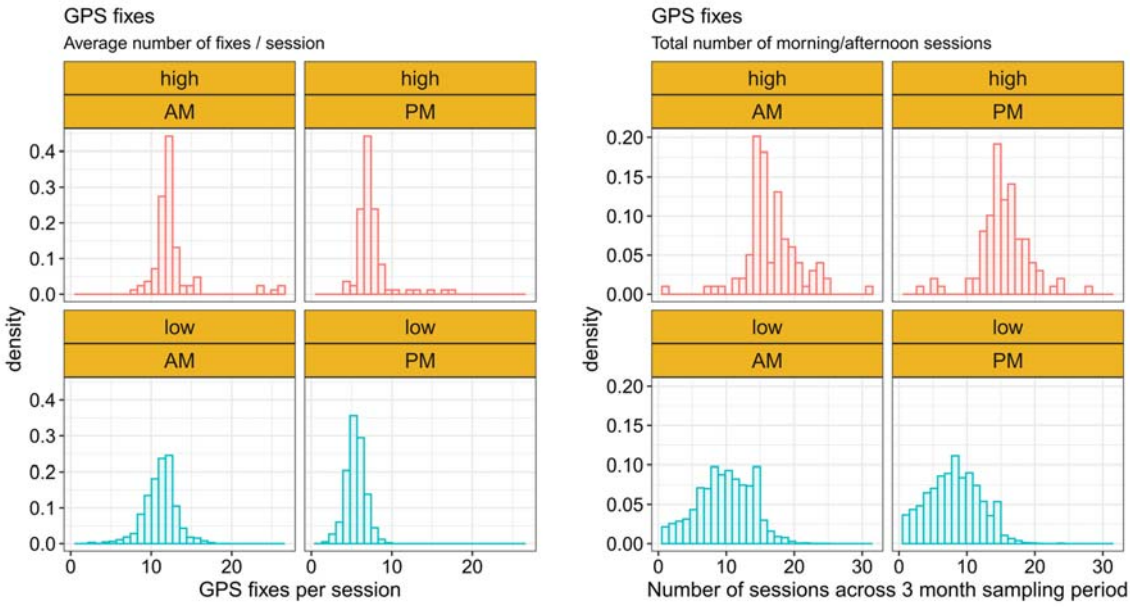

Figure S3.1. Variation in sampling effort for the 3-month periods of GPS data, separated by high resolution and low-resolution periods. The 100 periods providing the most GPS points were classed as high resolution, all others were low resolution. Each plot displays the density distribution data of the number of GPS fixes per sessions (left) or the total number of sessions (right) for both high- and low-resolution subsets of the data and for morning and evening sessions.

To conduct the sensitivity analysis, we first ranked all three-month periods in the population according to the total number of GPS that were points taken while the group was foraging. Plotting the cumulative sampling effort of the top 100 periods indicated that the top 9 periods had unusually high sampling rates (and appear in the right-hand tail mentioned above). These periods were excluded from the resampling procedure as they were unrepresentative (Figure S3.2). The next 50 most data-rich periods were then taken forward and used: ranks 10-59. For each of these periods, we randomly sampled 5, 10, 15, 20, 30, 40, 50 or sessions from the period, and repeated this process 50 times, resulting in a total of 50 random samples for each sample size and for each period. The home range for each random sample was estimated as the kernel density estimate (KDE) and the autocorrelated KDE (aDKE) using the `ctmm` package in R (Fleming & Calabrese, 2022), before all the results were collated.

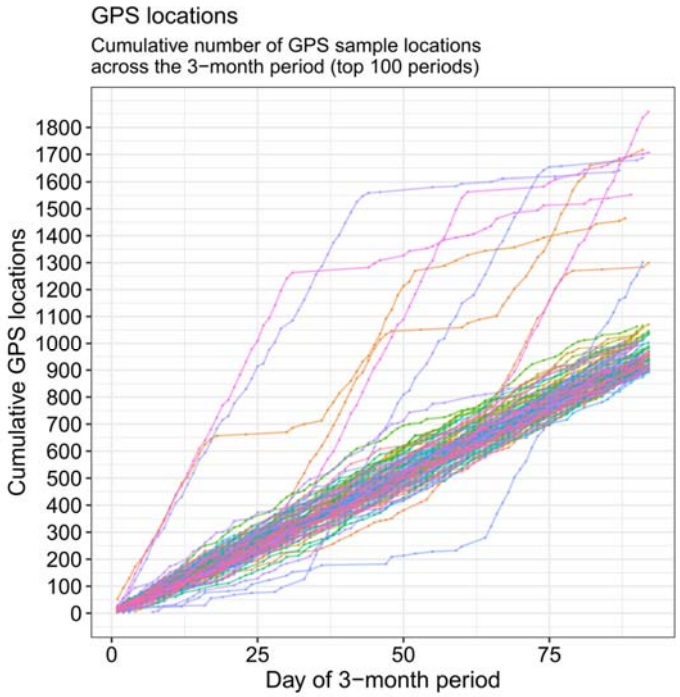

Figure S3.2. The cumulative sampling effort through time for the hundred three-month periods providing the most GPS data. The unusual sampling dynamics of the 9 periods providing the most data was used as justification for their exclusion from the sensitivity analysis.

In general, the sensitivity analysis shows that once groups were visited around 20 times within a three-month period, the size of their utilisation distributions (UD-50%, UD-75% & UD95%) began to plateau. This means that home ranges estimated from greater than or equal to 20 session visits can be considered to provide fairly accurate measures of longer-term space use. There will of course be exceptions, such as if groups show a sudden home range shift. But providing that any given group remains in roughly the same area for three-months, and providing that they are visited in each month of the three-month period, then 20 visits is sufficient to regard the UDs as informative. With less than 20 visits, there is a strong chance that a group's total space use has been underestimated and that the UD's will be relatively smaller as a result.

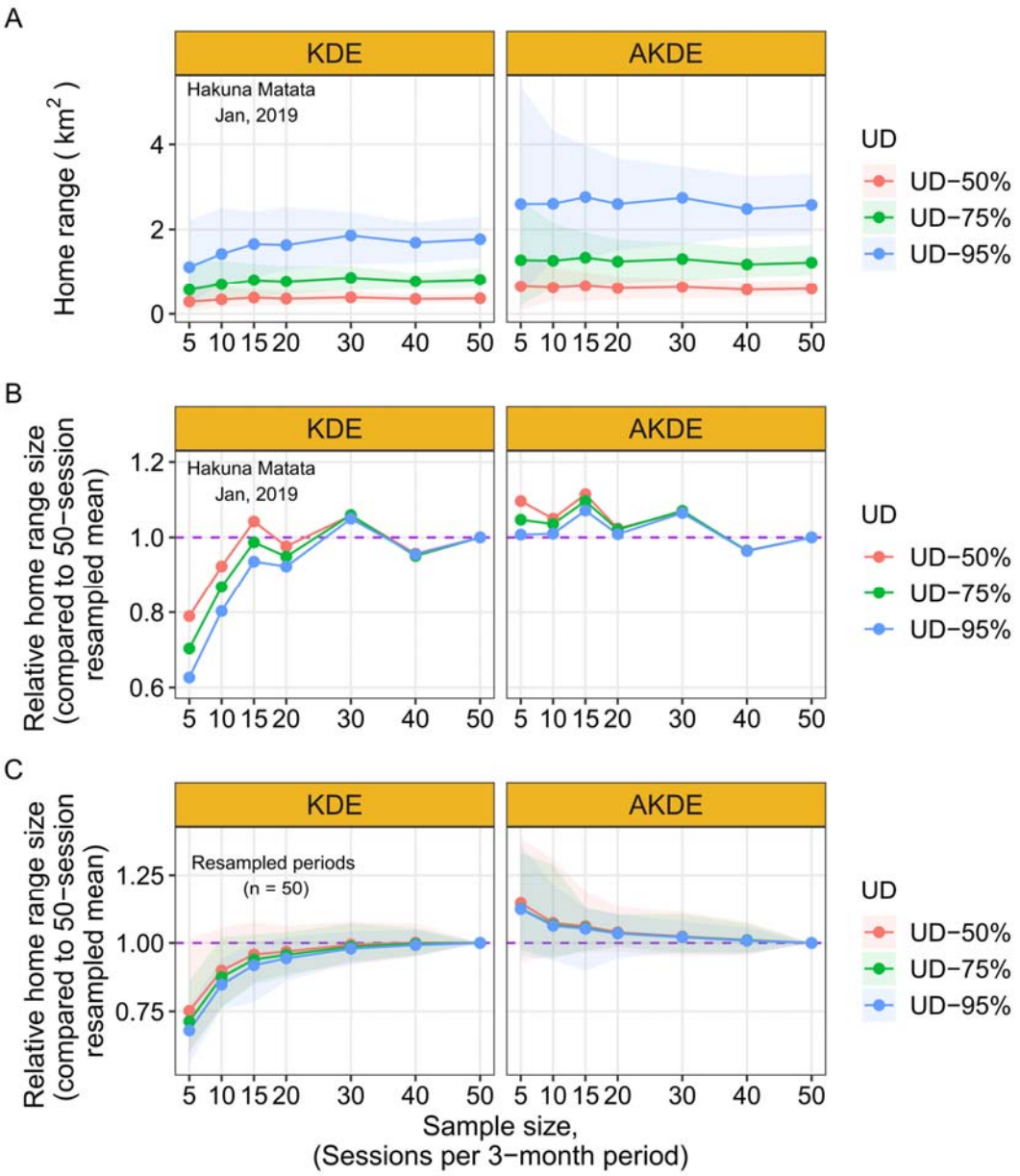

Figure S3.3. Sensitivity of home range size to sampling effort. (A) The upper panels display the effect of sampling effort on home range size for a single three-month period (for one group for three months). The sample size here refers to the number of sessions sampled from the original data, with 50 iterations performed at each increment. The points show the mean (± 95% CI) utilisation distribution at the 50%, 75% and 95% level across 50 resampling procedures, estimated using the kernel density estimate (KDE) or the autocorrelated kernel density estimate (aKDE). In the example, increases in sampling effort increased the size of the utilisation distributions (home range) and reduced their uncertainty at all levels. Around 20 sessions were required for the UDs to approach the 'large-sample' mean. (B) The middle panel re-plots the information in the upper panel as relative home range size, where the size of the UD-50%, UD-75% or UD-95% is calculated relative to the 50-sample mean. This provides a standardised measure of the effect of sampling effort on relative home range size. (C) When the sensitivity analysis is conducted on 50 distinct three-month periods, the effect of sampling effort on relative home range is displayed in the lower panels.

Section 4. The number of hot days in the Kalahari is increasing.

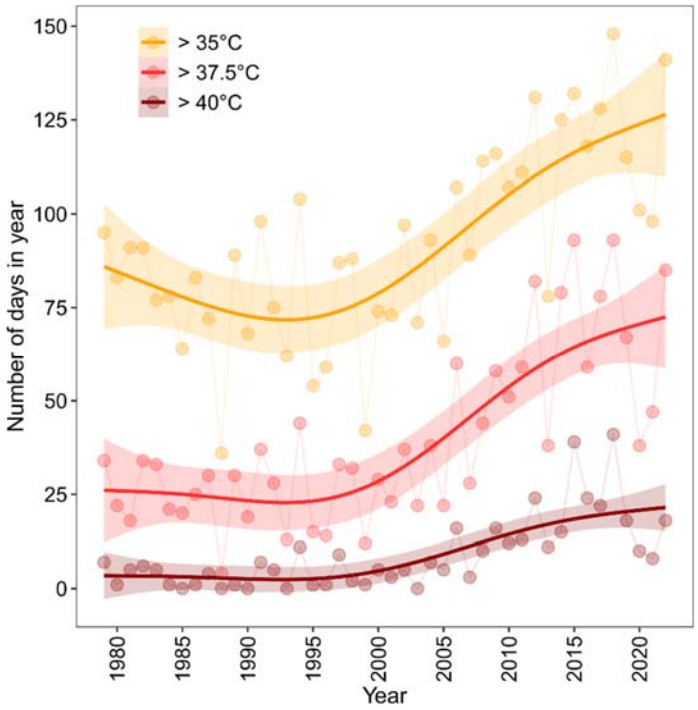

Figure S4.1. The number of days per year that air temperatures exceeded three different thresholds at our study site, since 1979. For each threshold the number of 'hot days', has risen dramatically since the 1990s. Points show the raw data, the solid lines show the predicted trends and their associated 95% confidence intervals (shaded area). The trendline for each threshold was estimated with a thin plate spine (k = 5). Temperature data came from NOAA's CPC product. The thresholds were determined from assays performed in captivity by Müller and Lojewski (1986), who found that the upper critical threshold for meerkats is around 33ºC, with significant evaporative water loss and the onset of panting occurring beyond 35ºC.

Section 5. Pregnancy rates and litters per year.

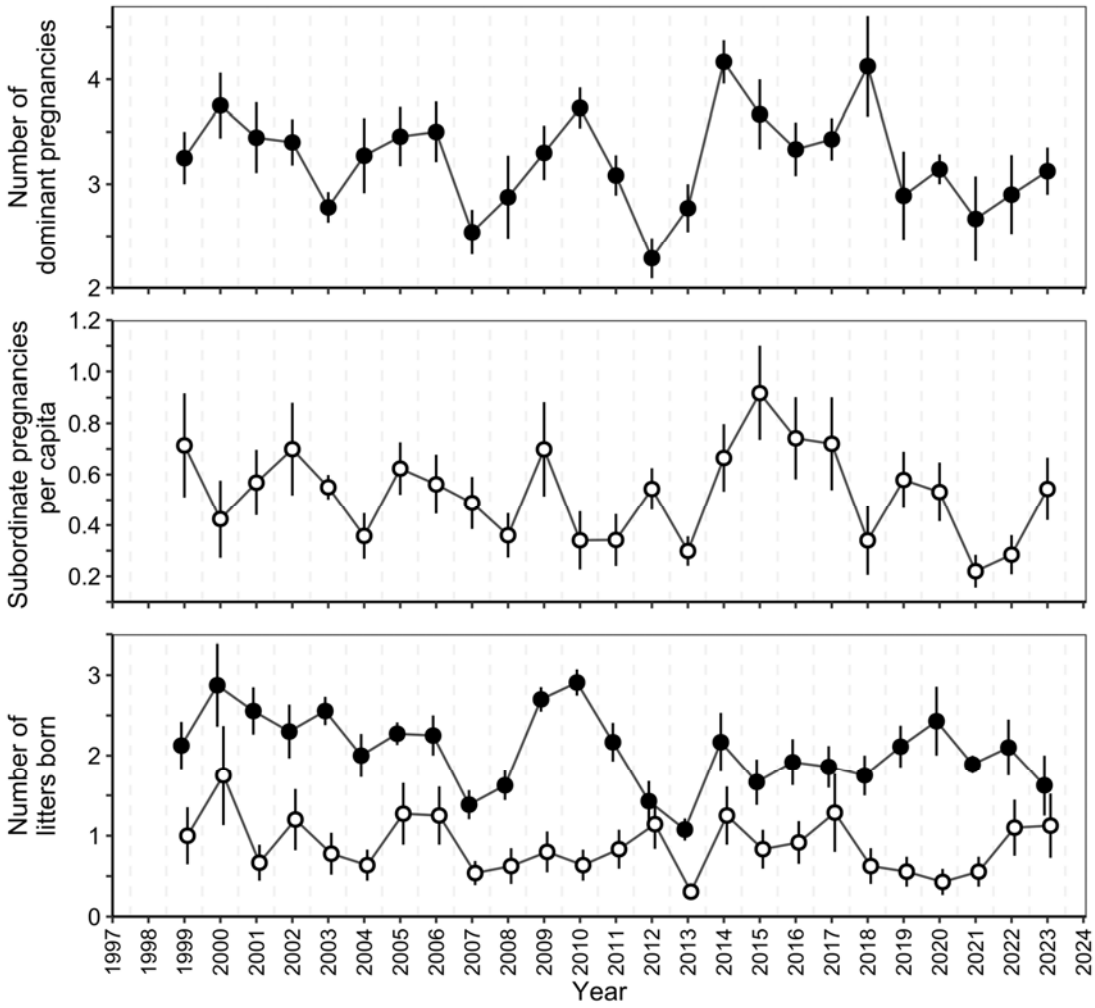

Figure S5.1. Annual rates of pregnancy in dominant and subordinate females, and the average number of litters born each year to dominant and subordinate females. Each metric is averaged over all groups in each year (mean ± SEM). On a per-capita basis, subordinate pregnancies showed a modest, non-significant decline (Kendall's tau, $z = -1.24$, $p = 0.22$, $\beta_{Sen} = -0.005$ [95%CI: -0.015, 0.005], $n = 25$; Figure S5.1B).

Section 6. Effects of climate on annual measures of reproduction and survival.

Table S6.1. Linear regression summaries and AICc ranking for models comparing the effects of climate variables on the mean number of dominant female pregnancies, mean number of litters born to dominant females, or the mean number of pups emerged or recruited from each group annually (1998-2023). Models were ranked by ΔAICc, which indicates the contrast from the most parsimonious model. We also present the standardised slopes (β) for each climate variable and their associated p-values, as well as the coefficient of determination (R^2) for each model. Detrended comparisons refers to models where predictor and responses variables were year-detrended before being modelled.

	Original					Detrended				
	Mean dom female pregnancies (n = 25 years)					**Mean dom female pregnancies (n = 25 years)**				
Climate variable	ΔAICc	Rank	β ± SE	R^2	p	ΔAICc	Rank	β ± SE	R^2	p
Null (~ 1 + group size)	0.57	2	-	0.12	-	0.00	1	-	0.20	-
Rainfall										
Early season rainfall (Sep-Nov)	1.59	5	0.12 ± 0.09	0.18	0.21	1.79	4	0.08 ± 0.09	0.23	0.34
Breeding season rainfall (Sep-Apr)	0.85	3	0.14 ± 0.09	0.20	0.14	1.24	2	0.10 ± 0.09	0.25	0.24
Combined two-year rainfall	2.87	8	0.07 ± 0.10	0.14	0.49	2.27	5	0.07 ± 0.09	0.22	0.48
Temperature										
Mean maximum summer temperature (Dec – Apr)	0.00	1	-0.17 ± 0.09	0.23	0.086	1.64	3	-0.09 ± 0.09	0.24	0.31
Mean maximum annual temperature (Jul – Jun)	0.93	4	-0.17 ± 0.11	0.20	0.14	2.73	7	-0.03 ± 0.10	0.20	0.74
SPEI										
Mean annual SPEI-6 (Jul-Jun)	2.77	7	0.08 ± 0.10	0.14	0.45	2.81	8	0.02 ± 0.09	0.20	0.84
Combined two-year mean SPEI-6	2.45	6	0.11 ± 0.12	0.15	0.36	2.72	6	0.04 ± 0.11	0.21	0.73

	Original					Detrended				
	Mean dom female litters (n = 25 years)					**Mean dom female litters (n = 25 years)**				
Climate variable	ΔAICc	Rank	β ± SE	R^2	p	ΔAICc	Rank	β ± SE	R^2	p
Null (~ 1 + group size)	8.07	6	-	0.00	-	6.16	3	-	0.06	-
Rainfall										
Early season rainfall (Sep-Nov)	7.85	5	0.16 ± 0.09	0.12	0.10	7.17	5	0.11 ± 0.09	0.12	0.21
Breeding season rainfall (Sep-Apr)	0.00	1	0.28 ± 0.08	0.35	0.002	0.00	1	0.23 ± 0.07	0.34	0.005
Combined two-year rainfall	8.29	8	0.16 ± 0.10	0.10	0.13	5.87	2	0.16 ± 0.09	0.17	0.10
Temperature										
Mean maximum summer temperature (Dec – Apr)	4.80	3	-0.23 ± 0.09	0.22	0.021	7.00	4	-0.12 ± 0.09	0.13	0.19
Mean maximum annual temperature (Jul – Jun)	4.45	2	-0.27 ± 0.11	0.23	0.018	7.83	7	-0.10 ± 0.10	0.10	0.31
SPEI										
Mean annual SPEI-6 (Jul-Jun)	7.50	4	0.19 ± 0.10	0.13	0.086	7.67	6	0.10 ± 0.09	0.10	0.28
Combined two-year mean SPEI-6	8.14	7	0.20 ± 0.13	0.11	0.12	8.22	8	0.09 ± 0.11	0.08	0.41

Table 6.1 continued…

	Original					Detrended				
	Mean pups emerged per group (n = 25 years)					**Mean pups emerged per group (n = 25 years)**				
Climate variable	ΔAICc	Rank	β ± SE	R^2	p	ΔAICc	Rank	β ± SE	R^2	p
Null (~ 1 + group size + group size^2)	14.28	6	-	0.30	-	5.64	4	-	0.25	-
Rainfall										
Early season rainfall (Sep-Nov)	16.08	8	0.53 ± 0.49	0.33	0.29	8.06	7	0.40 ± 0.51	0.27	0.44
Breeding season rainfall (Sep-Apr)	0.00	1	1.60 ± 0.35	0.65	<0.001	0.00	1	1.25 ± 0.42	0.47	0.007
Combined two-year rainfall	9.72	2	1.28 ± 0.46	0.48	0.012	5.00	2	0.95 ± 0.51	0.35	0.077
Temperature										
Mean maximum summer temperature (Dec – Apr)	10.51	3	-1.17 ± 0.45	0.47	0.017	5.02	3	-0.86 ± 0.47	0.35	0.078
Mean maximum annual temperature (Jul – Jun)	13.57	5	-1.03 ± 0.55	0.40	0.075	4.73	5	-0.72 ± 0.53	0.31	0.19
SPEI										
Mean annual SPEI-6 (Jul-Jun)	13.51	4	0.95 ± 0.51	0.40	0.073	7.47	6	0.55 ± 0.51	0.28	0.30
Combined two-year mean SPEI-6	15.91	7	-0.75 ± 0.65	0.34	0.26	8.76	8	0.11 ± 0.60	0.25	0.85

	Original					Detrended				
	Mean pups recruited per group (n = 25 years)					**Mean pups recruited per group (n = 25 years)**				
Climate variable	ΔAICc	Rank	β ± SE	R^2	p	ΔAICc	Rank	β ± SE	R^2	p
Null (~ 1 + group size + group size^2)	24.74	8	-	0.15	-	13.37	5	-	0.18	-
Rainfall										
Early season rainfall (Sep-Nov)	24.24	7	0.96 ± 0.53	0.27	0.083	14.19	7	0.74 ± 0.51	0.26	0.17
Breeding season rainfall (Sep-Apr)	0.00	1	2.11 ± 0.32	0.72	<0.001	0.00	1	1.67 ± 0.38	0.58	<0.001
Combined two-year rainfall	17.45	3	1.65 ± 0.50	0.44	0.003	8.84	2	1.35 ± 0.49	0.40	0.012
Temperature										
Mean maximum summer temperature (Dec – Apr)	16.05	2	-1.66 ± 0.47	0.47	0.002	10.90	3	-1.07 ± 0.47	0.35	0.032
Mean maximum annual temperature (Jul – Jun)	19.74	5	-1.64 ± 0.58	0.39	0.010	13.68	6	-0.87 ± 0.55	0.27	0.13
SPEI										
Mean annual SPEI-6 (Jul-Jun)	19.35	4	1.53 ± 0.52	0.40	0.008	12.73	4	0.94 ± 0.51	0.30	0.078
Combined two-year mean SPEI-6	22.65	6	1.51 ± 0.68	0.31	0.038	15.35	8	0.62 ± 0.61	0.22	0.32

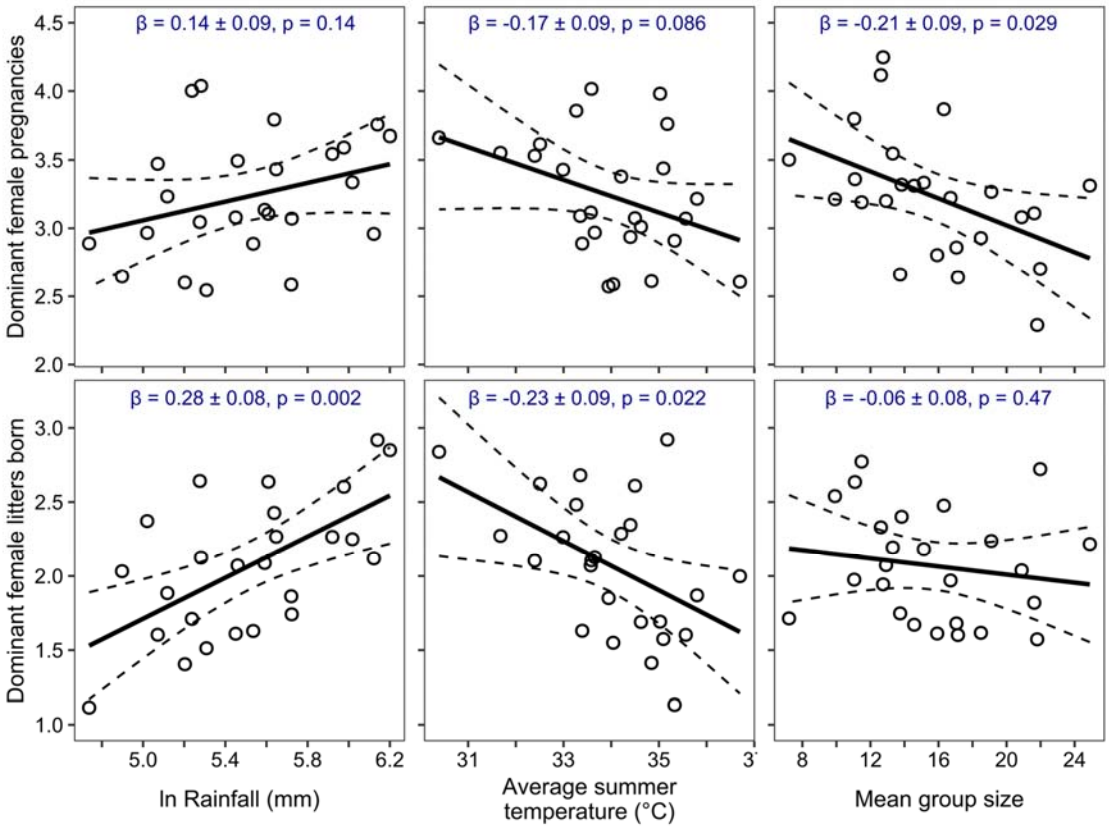

Figure S6.1. Effects of climate variables and group size on the mean number of dominant female pregnancies (upper) and litters born (lower) per year, averaged over all groups. The slopes and their associated 95% confidence intervals display the predictions from multiple regressions. Rainfall represents the ln rainfall across the breeding season (Sep-Apr), whereas temperature represents the mean maximum summer temperature (Dec-Apr). Predictions for the effects of temperature and rainfall come from regressions that also included an effect of mean group size at the start of the year, and the predictions for the effects of mean group size come from regressions that included temperature. Points are displayed as partial residuals so that the effects of the focal variable can be seen independently of the other modelled terms.

Table S6.2. Linear regression summaries and AICc ranking for models comparing the effects of different climate variables on the mean annual survival of pups and non-pups across all groups (1998-2023). Models were ranked by the change in AICc (ΔAICc), which indicates the contrast from the most parsimonious model. We also present the standardised slopes (β) for each climate variable and their associated p-values, as well as the coefficient of determination (R^2) for each model. Detrended comparisons refers to models where predictor and responses variables were year-detrended before being modelled.

	Normal					Detrended				
	Mean **pup survival** per group (n = 25 years)					Mean **pup survival** per group (n = 25 years)				
Climate variable	ΔAICc	Rank	β ± SE	R^2	p	ΔAICc	Rank	β ± SE	R^2	p
Null (~ 1+ group size)	17.12	8	-	0.02	-	16.31	6	-	0.02	-
Rainfall										
Early season rainfall (Sep-Nov)	9.60	3	0.062 ± 0.019	0.35	0.003	10.12	3	0.049 ± 0.016	0.32	0.005
Breeding season rainfall (Sep-Apr)	0.00	1	0.079 ± 0.015	0.56	<0.001	0.00	1	0.065 ± 0.013	0.64	<0.001
Combined two-year rainfall	11.96	5	0.061 ± 0.021	0.29	0.009	7.67	2	0.059 ± 0.016	0.44	0.002
Temperature										
Mean maximum summer temperature (Dec – Apr)	9.51	2	-0.065 ± 0.019	0.35	0.003	15.06	5	-0.035 ± 0.018	0.17	0.060
Mean maximum annual temperature (Jul – Jun)	11.03	4	-0.071 ± 0.023	0.31	0.006	18.02	8	-0.021 ± 0.021	0.06	0.32
SPEI										
Mean annual SPEI-6 (Jul-Jun)	12.06	6	0.062 ± 0.022	0.29	0.009	14.67	4	0.038 ± 0.018	0.18	0.049
Combined two-year mean SPEI-6	14.11	7	0.065 ± 0.027	0.22	0.025	16.62	7	0.033 ± 0.022	0.11	0.14

	Normal					Detrended				
	Mean **non-pup survival** per group (n = 25 years)					Mean **non-pup survival** per group (n = 25 years)				
Climate variable	ΔAICc	Rank	β ± SE	R^2	p	ΔAICc	Rank	β ± SE	R^2	p
Null (~ 1+ group size)	0.00	1	-	0.42	-	0.00	1	-	0.31	-
Rainfall										
Early season rainfall (Sep-Nov)	1.66	6	0.013 ± 0.013	0.45	0.31	2.16	4	0.010 ± 0.012	0.33	0.44
Breeding season rainfall (Sep-Apr)	0.97	3	0.017 ± 0.013	0.47	0.20	1.69	2	0.013 ± 0.012	0.34	0.32
Combined two-year rainfall	2.37	8	0.010 ± 0.014	0.43	0.52	2.39	6	0.009 ± 0.014	0.32	0.53
Temperature										
Mean maximum summer temperature (Dec – Apr)	1.00	4	-0.017 ± 0.013	0.46	0.21	2.27	5	-0.009 ± 0.013	0.33	0.47
Mean maximum annual temperature (Jul – Jun)	0.90	2	-0.021 ± 0.015	0.47	0.19	2.45	7	-0.008 ± 0.014	0.32	0.55
SPEI										
Mean annual SPEI-6 (Jul-Jun)	1.11	5	0.018 ± 0.014	0.46	0.22	1.99	3	0.012 ± 0.013	0.33	0.39
Combined two-year mean SPEI-6	1.76	7	0.017 ± 0.017	0.45	0.33	2.47	8	0.009 ± 0.015	0.32	0.56

Table S6.3. Linear regression summaries and AICc ranking for models comparing the effects of different climate variables on the mean annual survival of juveniles and subadults (combined), and adults, across all groups (1998-2023). Models were ranked by the change in AICc (ΔAICc), which indicates the contrast from the most parsimonious model. We also present the standardised slopes (β) for each climate variable and their associated p-values, as well as the coefficient of determination (R^2) for each model. Detrended comparisons refers to models where predictor and response variables were year-detrended before model fitting.

	Normal					Detrended				
	Mean **juvenile + subadult** survival per group (n = 25 years)					Mean **juvenile + subadult** survival per group (n = 25 years)				
Climate variable	ΔAICc	Rank	β ± SE	R^2	p	ΔAICc	Rank	β ± SE	R^2	p
Null (~ 1+ group size)	3.82	6	-	0.35	-	2.45	5	-	0.23	-
Rainfall										
Early season rainfall (Sep-Nov)	3.05	5	0.029 ± 0.015	0.44	0.077	2.51	6	0.024 ± 0.015	0.31	0.12
Breeding season rainfall (Sep-Apr)	2.39	3	0.031 ± 0.015	0.45	0.055	2.07	3	0.026 ± 0.015	0.33	0.096
Combined two-year rainfall	5.67	8	0.017 ± 0.018	0.37	0.35	4.29	7	0.016 ± 0.017	0.26	0.35
Temperature										
Mean maximum summer temperature (Dec – Apr)	0.00	1	-0.039 ± 0.015	0.50	0.017	0.24	2	-0.032 ± 0.14	0.37	0.037
Mean maximum annual temperature (Jul – Jun)	1.38	2	-0.041 ± 0.018	0.47	0.033	0.00	1	-0.036 ± 0.016	0.38	0.033
SPEI										
Mean annual SPEI-6 (Jul-Jun)	2.45	4	0.034 ± 0.017	0.45	0.056	2.37	4	0.026 ± 0.016	0.32	0.11
Two-year mean SPEI-6	4.84	7	0.028 ± 0.021	0.39	0.21	4.41	8	0.017 ± 0.019	0.26	0.38
	Normal					Detrended				
	Mean **adult** survival per group (n = 25 years)					Mean **adult** survival per group (n = 25 years)				
	ΔAICc	Rank	β ± SE	R^2	p	ΔAICc	Rank	β ± SE	R^2	p
Null (~ 1+ group size)	0.00	1	-	0.33	-	0.00	1	-	0.23	-
Rainfall										
Early season rainfall (Sep-Nov)	2.83	8	0.002 ± 0.015	0.33	0.88	2.85	8	-0.001 ± 0.014	0.23	0.93
Breeding season rainfall (Sep-Apr)	2.71	6	0.005 ± 0.015	0.34	0.72	2.84	7	0.002 ± 0.014	0.23	0.92
Combined two-year rainfall	2.75	7	0.005 ± 0.016	0.34	0.76	2.77	4	0.004 ± 0.015	0.23	0.78
Temperature										
Mean maximum summer temperature (Dec – Apr)	2.65	5	-0.006 ± 0.015	0.34	0.67	2.82	5	0.003 ± 0.014	0.23	0.86
Mean maximum annual temperature (Jul – Jun)	2.41	3	-0.011 ± 0.018	0.34	0.53	2.73	3	0.005 ± 0.016	0.23	0.74
SPEI										
Mean annual SPEI-6 (Jul-Jun)	2.55	4	0.008 ± 0.016	0.34	0.61	2.82	6	0.003 ± 0.015	0.23	0.86
Two-year mean SPEI-6	2.25	2	0.014 ± 0.019	0.35	0.47	2.68	2	0.007 ± 0.017	0.24	0.69

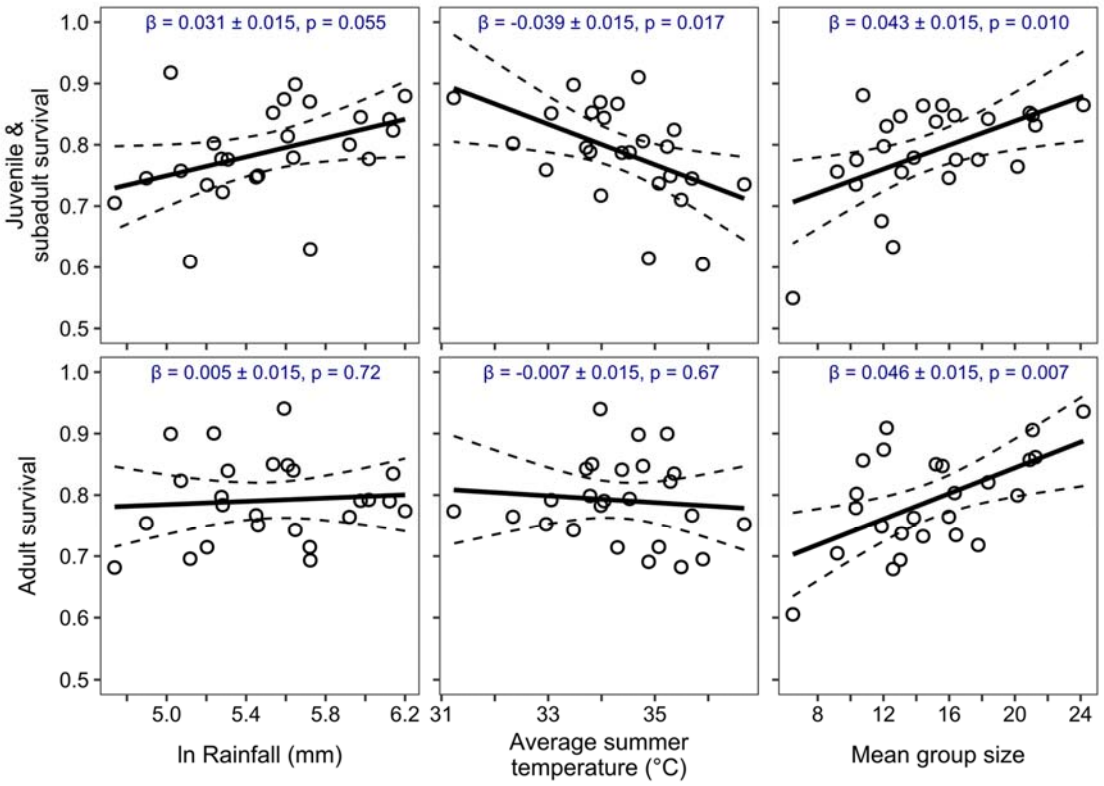

Figure S6.2. Effects of climate variables and group size on annual survival of juveniles and sub-adults (upper) and adults (lower), averaged over all groups. The slopes and their associated 95% confidence intervals display the predictions from multiple regressions. Rainfall represents the ln rainfall across the breeding season (Sep-Apr), whereas temperature represents the mean maximum summer temperature (Dec-Apr). Predictions for the effects of temperature and rainfall come from regressions that also included an effect of mean group size at the start of the year, and the predictions for the effects of mean group size come from regressions that included temperature. Points are displayed as partial residuals so that the effects of the focal variable can be seen independently of the other modelled terms.

Table S6.4. Testing the effects of temperature and rainfall in the same multiple regressions. For each response variable, we compared a full additive model (response ~ group size/density + rainfall + temperature) to the best supported nested model (response ~ group size/density + rainfall/temperature), where rainfall was always the total breeding season rainfall, and temperature was either the average maximum summer temperature, or the average maximum winter temperature, which ever explained more variation (See Table 2 in main text and Tables S6.1 to S6.3). The rainfall and temperature estimates represent the standardised slopes (β) for each variable and their associated p-values in the full model. ΔAICc and ΔR^2 indicate the change in Akaike's information criterion (corrected for small sample size) and the change in explained variation in the full model relative to the nested, simpler model.

Model	Response variable	Rainfall estimate (SE)	Rainfall p value	Temperature estimate (SE)	Temperature p value	ΔAICc	ΔR^2
i	Population density change	0.22 (0.06)	0.007	0.03 (0.06)	0.001	3.31	0.01
ii	Group size change	0.13 (0.05)	0.014	-0.03 (0.06)	0.60	2.84	0.01
iii	No. dominant female pregnancies	0.07 (0.11)	0.53	-0.12 (0.11)	0.29	2.67	0.02
iv	No. dominant female litters	0.22 (0.09)	0.018	-0.15 (0.11)	0.16	0.75	0.06
v	No. pups emerged	1.44 (0.43)	0.003	-0.31 (0.45)	0.50	2.93	0.01
vi	No. pups recruited	1.79 (0.38)	<0.001	-0.59 (0.40)	0.16	0.95	0.03
vii	Pup survival	0.065 (0.018)	0.002	-0.026 (0.019)	0.19	1.02	0.04
vii	Juvenile + subadult survival	0.014 (0.018)	0.45	-0.031 (0.019)	0.11	0.08	0.06
ix	Adult survival	0.002 (0.0017)	0.92	-0.010 (0.020)	0.61	3.15	0.00

Section 7. Long-term trends in adult body mass at different times of year.

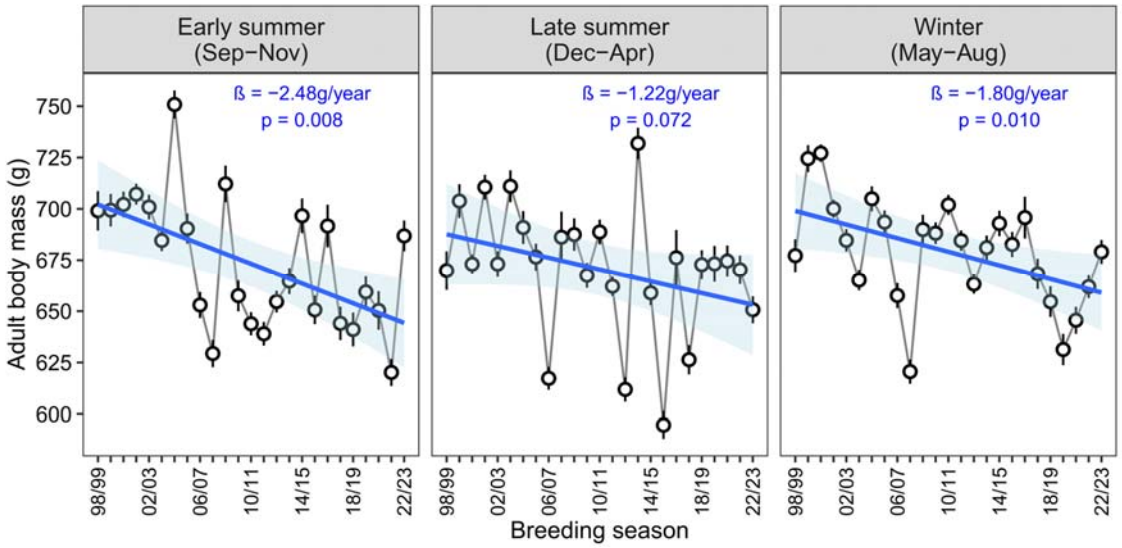

Figure S7.1. Variation in the average body mass of adult meerkats over time, separated by season. Each data point represents the average mean body mass of all adults weighed in the population in each season of the year (error bars: SEM). The linear rate of change was calculated as Sen's slope (β) and the significance of each decline was assessed via the non-parametric Mann-Kendall trend test. The blue slopes show the linear regression through the data.

Section 8. References

Fensholt, R., Rasmussen, K., Kasperson, P., Huber, S., Horion, S., and Swinnen, F. 2013. Assessing land degradation/recovery in the African Sahel from long-term Earth Observation based primary productivity and precipitation relationships. *Remote Sensing* 5(2): 664-686. https://doi.org/10.3390/rs5020664

Fleming, C. H., and Calabrese, J. M. 2022. ctmm: Continuous-time movement modeling. R package v1.1. https://CRAN.R-project.org/package=ctmm

Hufkens, K. 2022. The MODISTools package: an interface to the MODIS Land products subsets web services. https://github.com/ropensci/MODISTools

Huffman, G. J., Adler, R. F., Behrangi, A., Bolvin, D. T., Nelkin, E. J., Gu, G., and Reza Ehsani, M. 2023. The new version 3.2 Global Precipitation Climatology Project (GPCP) monthly and daily precipitation products. *Journal of Climate* 32(21): 7635-7655. https://doi.org/10.1175/JCLI-D-23-0123.1

Jönsson, P., and Eklundh, L. 2004. TIMESAT- a program for analysing time-series of satellite sensor data. *Computers and Geosciences* 30(8): 833-845. https://doi. org/10.1016/j.cageo.2004.05.006

Kranstauber, B., Gall, G. E. C., Vink, T., Clutton-Brock, T., and Manser, M. B. 2019. Long-term movements and home-range changes: rapid territory shifts in meerkats. *Journal of Animal Ecology* 89(3): 772-783. https://doi.org/10.1111/1365-2656.13129

Müller, E. F., and Lojewski, U. 1986. Thermoregulation in the meerkat (*Suricata suricatta* schreber, 1776). *Comparative Biochemistry and Physiology Part A: Physiology* 83: 217–224. https://doi.org/10.1016/0300-9629(86)90564-5

Ogle, K, Reynolds, J. F. 2004. Plant responses to precipitation in desert ecosystems: integrating functional types, pulses, thresholds, and delayed. *Oecologia* 141: 282-294. https://doi.org/10.1007/s00442-004-1507-5

Tokura, W., Jack, S. L., Anderson, T., and Hoffman, M. T. 2018. Long-term variability and vegetation productivity in relation to rainfall, herbivory, and fire in Tswalu Kalahari Reserve. *Koedoe* 60(1): a1473. https://doi.org/10.4102/koedoe.v60i1.1473

Turbé, A. 2006. Foraging decisions and space use in a social mammal, the meerkat. PhD Thesis, University of Cambridge.

Wessels, K., Steenkamp, K., von Maltitz, G., and Archibald, S. 2011. Remotely sensed vegetation phenology for describing and predicting the biomes of South Africa. *Applied Vegetation Science* 14(1): 49-66. https://doi.org/10.1111/j.1654-109X. 2010.01100.x